Acta Crystallographica Section B
Structural Science
ISSN 0108-7681

Solid-state compounds of stereoisomers: *cis* and *trans* isomers of 1,2-cyclohexanediol and 2,3-tetralindiol

Michael A. Lloyd, Garth E. Patterson, Greg H. Simpson, Laura L. Duncan, Daniel P. King, Yigang Fu, Brian O. Patrick, Sean Parkin and Carolyn Pratt Brock*

Department of Chemistry, University of Kentucky, Lexington, KY 40506-0055, USA

Correspondence e-mail: cpbrock@uky.edu

Received 4 October 2006
Accepted 5 March 2007

The phases of 1,2,3,4-tetrahydro-2,3-naphthalenediol (or 2,3-tetralindiol) and of 1,2-cyclohexanediol have been investigated. The structure of a very stable 1:1 compound (or co-crystal) of the *cis* and *trans* isomers of 2,3-tetralindiol, the existence of which has been known for nearly a century, has finally been determined. No evidence of any analogous compound between the *cis* and *trans* isomers of 1,2-cyclohexanediol has been found. The formation of solid-state compounds of stereoisomers is rare; it probably occurs only if the crystal packing of at least one of the isomers is unfavorable, *e.g.* if at least one of the melting points is lower than expected. Compound formation is usually unlikely because of the difficulty of simultaneously optimizing the translational spacings for both isomers, but that packing problem is avoided in the *cis*/*trans* compound of 2,3-tetralindiol because the two isomers are in very similar environments. In the structures of the individual 2,3-tetralindiol isomers there are clear conflicts between the competing packing requirements of the 1,2-diol moiety and the aromatic ring system; these conflicts are resolved better in the co-crystal than in the structures of the individual isomers.

1. Introduction

What crystals can be expected to precipitate from a solution that is equimolar in two solutes? The formation of a solid-state compound is expected if an acid–base reaction (*e.g.* protonation of an amine by a strong acid) or an oxidation–reduction reaction (*e.g.* to yield a $D^{+}\cdot A^{-}$ salt) can occur. The ionic interactions in the product crystals account for their stability relative to crystals of the pure components.

Compound formation is no surprise if partial transfer of protons or electrons can take place, at least as long as the remaining parts of the molecules are compatible. Electronic donor:acceptor complexes have been known for many years (Herbstein, 1971). The use of hydrogen-bonding interactions to raise the probability of compound formation was pioneered by Etter (1990, 1991). The field of crystal engineering relies on the phenomenon of compound formation. Herbstein's recent two-volume treatise *Crystalline Molecular Complexes and Compounds* (Herbstein, 2005) provides a very comprehensive review.

Compound formation is likewise expected if the two compounds are enantiomers (see, *e.g.* Jacques *et al.*, 1981; Brock *et al.*, 1991; Herbstein, 2005). The D:L interactions are no different in kind from the D:D and L:L interactions, but the possibility of crystallization in a space group that includes an inversion center, which is known to be favorable for crystal packing (see Brock *et al.*, 1991; Patrick & Brock, 2006), is important enough that spontaneous resolution occurs less

Table 1
Phases known for 2,3-tetralindiol.

	T_{fus} (K)	Reference(s) for T_{fus}	Reference(s) for structure, REFCODE, T
cis	397–398	Verkade *et al.* (1928)	Klein *et al.* (1983), BOPRIH10, *ca* 293 K
	391	Lettré & Lerch (1952)	
	397	Ali & Owen (1958)	
rac	408–409	Verkade *et al.* (1928)	Unknown
	407	Lettré & Lerch (1952)	
	408–409	Ali & Owen (1958)	
	408	Brianso (1976)	
R,*R* or *S*,*S*	425	Lettré & Lerch (1952)	Brianso (1976), TETRDO, *ca* 293 K
	436	Brianso (1976)	Lloyd *et al.* (1998), TETRDO01, *ca* 293 K
1:1 *cis*/*rac-trans*	414–415	Verkade *et al.* (1928)	This work
	413	Lettré & Lerch (1952)	
1:1 *cis*/*R*,*R* (or 1:1 *cis*/*S*,*S*)	422	Lettré & Lerch (1952)	

than *ca* 10% of the time (see references cited above). The presence of improper symmetry elements very greatly increases the number of possible relative orientations of adjacent molecules.

On the other hand, fractional crystallization is expected to be successful in the general case of precipitation from a solution equimolar in two unrelated solute molecules *A* and *B*; the precipitate is expected to be composed of crystals of *A* and crystals of *B* except in the special cases noted above. In most cases the types of attractive interactions in which *A* and *B* molecules (or sets of ions) participate are sufficiently different that the formation of a solid-state compound (*i.e.* of a co-crystal) would be a surprise.

Separation is then anticipated if molecules *A* and *B* are stereoisomers; it is assumed that they can be separated by fractional crystallization. But what is the basis for that assumption? Stereoisomers have the same functional groups; *A*:*B* interactions should be about as favorable as the average of *A*:*A* and *B*:*B* interactions. The isomers have different shapes, but Pauling & Delbrueck (1940) pointed out that it is the complementarity of molecules rather than their identity that determines whether they will crystallize together. It is possible, however, that one reason few co-crystals of stereoisomers have been found is that few efforts have been made to look for them. Crystals of an *A*:*B* compound may easily escape notice if their melting point is similar to the eutectic temperature of a mixture of *A* and *B*, or if the melting points of *A* and *B* are sufficiently different that an *A*/*B* compound would appear in the *T*–*X* phase diagram as a peritectic point. Furthermore, it is unusual for crystals to be grown from solutions that are even approximately equimolar in two or more isomers.

A 1:1 compound formed from the *cis* and *trans* isomers of 1,2,3,4-tetrahydronaphthalene-2,3-diol (or 2,3-tetralindiol; hereafter, 2,3-TD) has been known since the beginning of the 20th century (see Leroux, 1909). While the structure of the 2,3-TD compound has never been published, a phase diagram for the system has (Lettré & Lerch, 1952). We decided to study 2,3-TD and as well as the smaller 'submolecule' 1,2-cyclohexanediol (hereafter, 1,2-CHD) in order to understand why the known *cis*/*trans* compound of 2,3-TD forms and to explore the more general question of the probability of compound formation between stereoisomers. The 2,3-TD and 1,2-CHD

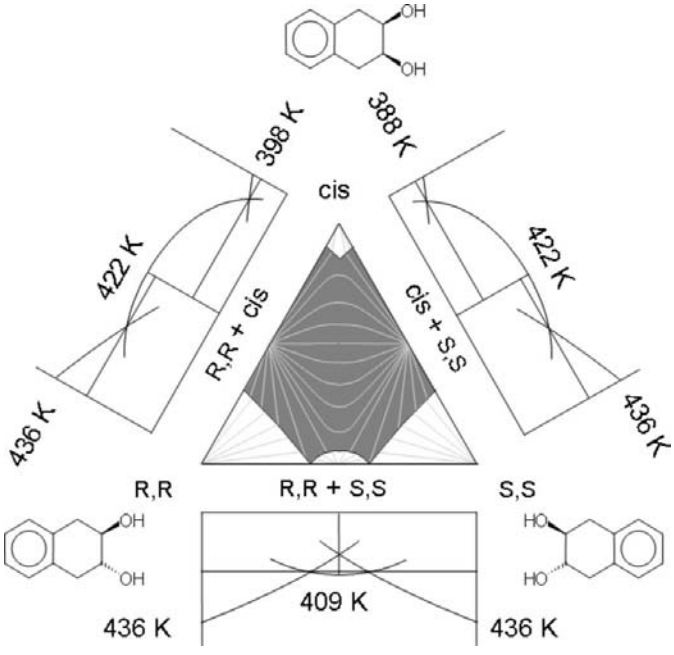

Figure 1
Schematic three-component *T*–*X* phase diagram for 2,3-tetralindiol drawn primarily from the data of Lettré & Lerch (1952); schematic *T*–*X* diagrams for each pair of components are also shown. The temperatures given are the highest values for each phase (see Table 1). The area corresponding to the phase containing both the *cis* and *trans* isomers is darkened. The two-component diagrams for the *cis* and enantiomerically pure components have been simplified; Lettré & Lerch (1952) indicate (see their Fig. 3) that in the nominal 1:1 phase of *cis* and *R*,*R*- (or *S*,*S*-) *trans* isomers some of the *trans* molecules may be replaced by *cis* molecules.

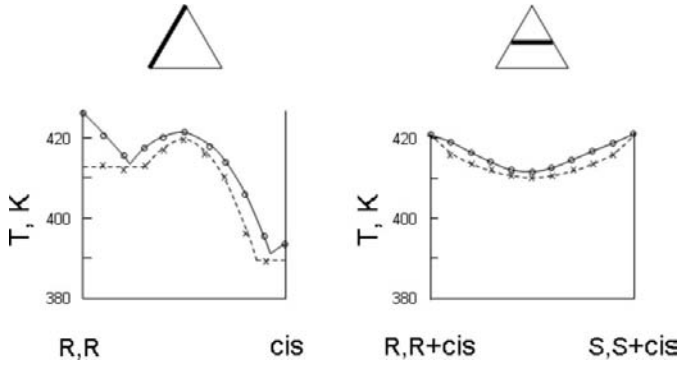

Figure 2
Details of two edges of the three-component phase diagram of 2,3-tetralindiol (see Fig. 1) as redrawn from the paper of Lettré & Lerch (1952).

Table 2
Phases known for 1,2-cyclohexanediol.

	T_{fus} (K)	Reference(s) for T_{fus}	Reference(s) for structure; REFCODE, *T*
cis	370–372	Verkade *et al.* (1928)	Sillanpää *et al.* (1984), ZZZPSA01, *ca* 293 K
	370	Lettré & Lerch (1952)	
rac	376–377	Verkade *et al.* (1928)	Sillanpää *et al.* (1984), ZZZKPE01, *ca* 293 K
	377	Lettré & Lerch (1952), Leitão *et al.* (2002)	Jones *et al.* (1989), ZZZKPE02, *ca* 293 K
	377	White (1931)	This work
	371	Leitão *et al.* (2002)	
R,*R*- or *S*,*S*-*trans*	384	Leitão *et al.* (2002)	Hanessian *et al.* (1994), PIWXIK, 215 K This work
cis/*rac*-*trans* mixture	345–346	Leroux (1909), White (1931)	Conglomerate
	344	Lettré & Lerch (1952)	

sets of isomers have been investigated in tandem by several sets of previous authors (Leroux, 1909; Verkade *et al.*, 1928; White, 1931; Lettré & Lerch, 1952).

2. Summary of known phases

The *R*,*R* and *S*,*S* forms of *trans*-2,3-TD and *trans*-1,2-CHD are separable enantiomers, but the *cis* isomer is a *meso* compound. The three different forms of the 1,2-cyclohexanediol ring are shown in (II): Schematic phase diagrams for 2,3-TD and 1,2-CHD as drawn from information available in the literature are given in Figs. 1–3.

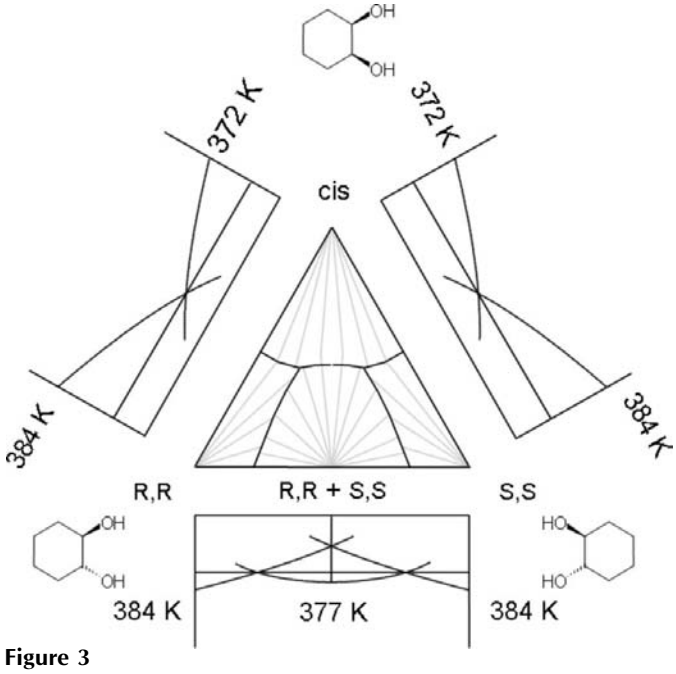

Figure 3
Schematic three-component *T*–*X* phase diagram for 1,2-cyclohexanediol drawn from the data shown in Table 2; schematic *T*–*X* diagrams for each pair of components are also shown. The temperatures given are the highest values for each phase. No phase containing both *cis* and *trans* isomers is known.

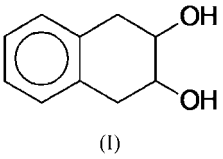

(I)

2.1. 2,3-Tetralindiols

Literature values for the melting points of the 2,3-TD phases and references to their structures and are summarized in Table 1; the refcodes in the Cambridge Structural Database (hereafter, the CSD; Allen, 2002) are also given. The most complete thermodynamic study was made by Lettré & Lerch (1952), who determined the complete three-component *T*–*X* phase diagram (see Figs. 1 and 2).

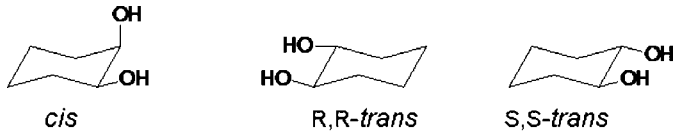

(II)

The 1:1 *cis*/*trans* compound of 2,3-TD is remarkably stable relative to the pure *cis* and *trans* isomers; this 1:1 compound[1] dominates the phase diagram. The estimated eutectic temperature (see *e.g.* Brock *et al.*, 1991) of the *cis* and *rac* (*i.e.* *rac*-*trans*)[2] isomers is 373 K, *i.e.* *ca* 40 K lower than the melting point of their 1:1 compound.

Crystals of *rac*-2,3-TD are reported to be only marginally more stable than crystals of the pure enantiomers. The eutectic temperature of the *R*,*R*- (or *S*,*S*-) and *rac*-2,3-TD crystals is no more than 5 K lower than T_{fus} for *rac*-2,3-TD (Lettré & Lerch, 1952; Brianso, 1976).

2.2. 1,2-Cyclohexanediols

Literature values for the melting points of the 1,2-CD phases and references to their structures are summarized in Table 2. The solid–liquid, *T*–*X* phase diagram of the *R*,*R* and *S*,*S* enantiomers has been determined recently (Leitão *et al.*, 2002; see the bottom part of Fig. 3).

Leroux (1909) and White (1931) gave the melting point of the 1:1 *cis*–*trans* mixture as 345–346 K, which is close to the eutectic temperature estimated for the *cis* + *rac* mixture.

[1] Lettré & Lerch (1952) demonstrated that the 1:1 'compound' of *cis*- and *rac*-2,3-tetralindiol corresponds to a minimum in the temperature curve when X_{cis} is 0.5 and $X_{S,S} = X_{R,R} = 0.25$. The 1:1 *cis*- and *rac*-2,3-tetralindiol 'compound' is therefore usually a mixed crystal (or solid solution) of 1:1 *cis*-2,3-TD/*R*,*R*-2,3-TD and *cis*-2,3-TD/*S*,*S*-2,3-TD. The term compound will, however, be used in what follows without quotation marks.

[2] Nomenclature rules call for leaving out the *trans* identifier for these compounds when *rac*, *R*,*R* or *S*,*S* is used because all three imply a *trans* arrangement of the hydroxyl substituents. We have occasionally violated that rule in the interest of clarity.

Table 3
Experimental data for 2,3-tetralindiol structures.

	1:1 *cis*/*trans*-2,3-TD	*S*,*S*-2,3-TD
Crystal data		
Chemical formula	$C_{10}H_{12}O_2{\cdot}C_{10}H_{12}O_2$	$C_{10}H_{12}O_2$
M_r	328.40	164.20
Cell setting, space group	Monoclinic, *C*121	Monoclinic, $P12_11$
Temperature (K)	90 (2)	90 (2)
a, *b*, *c* (Å)	23.2312 (13), 4.9750 (4), 15.484 (2)	5.8751 (2), 27.9972 (8), 5.0132 (2)
β (°)	112.53 (1)	94.528 (1)
V (Å^3)	1653.1 (3)	822.03 (5)
Z	4	4
D_x (Mg m^{-3})	1.311	1.327
Radiation type	Cu $K\alpha$	Cu $K\alpha$
μ (mm^{-1})	0.73	0.74
Crystal form, color	Thin blade (largest faces 001; elongated along [010]), colorless	Block, colorless
Crystal size (mm)	0.30 × 0.05 × 0.02	0.12 × 0.10 × 0.08
Data collection		
Diffractometer	Bruker–Nonius X8 Proteum	Bruker–Nonius X8 Proteum
Data collection method	ω and φ scans	ω and φ scans
Absorption correction	Multi-scan (based on symmetry-related measurements)	Multi-scan (based on symmetry-related measurements)
T_{min}	0.810	0.916
T_{max}	0.986	0.943
No. of measured, independent and observed reflections	10 614, 2316, 2226	9460, 2869, 2859
Criterion for observed reflections	$I > 2\sigma(I)$	$I > 2\sigma(I)$
R_{int}	0.116	0.029
θ_{max} (°)	66.4	68.0
Refinement		
Refinement on	F^2	F^2
$R[F^2 > 2\sigma(F^2)]$, $wR(F^2)$, S	0.079, 0.229, 1.18	0.036, 0.087, 1.12
No. of reflections	2316	2869
No. of parameters	239	222
H-atom treatment	Constrained to parent site	Constrained to parent site
Weighting scheme	$w = 1/[\sigma^2(F_o^2) + (0.111P)^2 + 7.930P]$, where $P = (F_o^2 + 2F_c^2)/3$	$w = 1/[\sigma^2(F_o^2) + (0.0573P)^2 + 0.1143P]$, where $P = (F_o^2 + 2F_c^2)/3$
$(\Delta/\sigma)_{max}$	< 0.0001	< 0.0001
$\Delta\rho_{max}$, $\Delta\rho_{min}$ (e Å^{-3})	0.44, −0.48	0.28, −0.30
Extinction method	None	*SHELXL*
Extinction coefficient	–	0.052 (2)
Absolute structure	–	Flack (1983)
Flack parameter	–	0.00 (13)

Computer programs used: *APEX2* (Bruker–Nonius, 2004), *Saintplus* in *APEX2* (Bruker–Nonius, 2004), *SHELXS97* (Sheldrick, 1997*a*), *SHELXL97* (Sheldrick, 1997*b*), *XP* in S*HELXTL* (Sheldrick, 1994), *Mercury* (Macrae *et al.*, 2006) and local procedures.

Leroux (1909) did claim the existence of a *cis*/*trans* compound, but Lettré & Lerch (1952) concluded that no such compound exists.

The estimated eutectic temperature (see *e.g.* Brock *et al.*, 1991) of the resolved *trans* enantiomers is 20–30 K lower than T_{fus} for the corresponding racemic compound, which means that the crystals of the resolved material are substantially less stable than the racemic crystals. The eutectic temperature of the racemic compound and one of its pure enantiomers appears to be ∼ 371 K (Leitão *et al.*, 2002).

The known crystal structures of *cis* and *rac*-1,2-CHD (refcode families ZZZPSA and ZZZKPE) are very similar; both are built from hydrogen-bonded layers of molecular dimers. The two unit cells have very similar dimensions and the same space group (*Pbca*). The possible existence of an additional polymorph of 1,2-CHD was raised by White (1931), who could not obtain the orthorhombic 'β' form (later identified as the *Pbca* structure) reported previously by Groth (1910). White identified a centered monoclinic unit cell containing eight molecules but did not know which isomer it contained; cell constants are given in the CSD under the entry ZZZKPE. The structure of this *C*2/*c* structure of *rac*-1,2-CHD is reported below. The two 1,2-CHD polymorphs contain hydrogen-bonded layers with the same pattern of hydrogen bonds, and their melting points seem to be very similar (see Table 2). We found the melting point of a sample that contained both polymorphs to be 374–377 K.

3. Structure determinations

Structures determined for the first time in this study are those of the 1:1 *cis*/*trans* compound of 2,3-TD (at 90 K) and the *C*2/*c* polymorph of *rac*-1,2-CHD (at 173 and 299 K). Also reported are the structure at 90 K of enantiomerically pure 2,3-TD and the structures at 173 K of the three 1,2-CHD structures known previously. New determinations of the four 1,2-CHD structures at room temperature and determinations of the enantiomerically pure 2,3-TD structure at 173 and 110 K are available in the supplementary material.[3]

Information about the determinations at 90 K of the two 2,3-TD structures is given in Table 3 and information about the determinations at 173 K of the four 1,2-CHD structures is found in Table 4. Additional information is given below. When data were collected with Mo radiation all *trans* isomers were chosen arbitrarily to be the *R*,*R* enantiomer (except for the minor component in the case of enantiomeric disorder). Near the end of the project we decided to collect data at 90 K for enantiomerically pure 2,3-TD and did so using Cu radiation from a rotating-anode

[3] Supplementary data for this paper are available from the IUCr electronic archives (Reference: WS5054). Services for accessing these data are described at the back of the journal.

Table 4
Experimental data for 1,2-cyclohexanediol structures.

	cis-1,2-CHD	*trans*-1,2-CHD polymorph 1	*trans*-1,2-CHD polymorph 2	*R*,*R*-1,2-CHD
Crystal data				
Chemical formula	$C_6H_{12}O_2$	$C_6H_{12}O_2$	$C_6H_{12}O_2$	$C_6H_{12}O_2$
M_r	116.16	116.16	116.16	116.16
Cell setting, space group	Orthorhombic, *Pbca*	Orthorhombic, *Pbca*	Monoclinic, *C*12/*c*1	Trigonal, $P3_221$
Temperature (K)	173 (2)	173 (2)	173 (2)	173 (2)
a, *b*, *c* (Å)	8.545 (2), 7.588 (1), 19.717 (4)	8.415 (1), 7.799 (1), 19.295 (2)	18.321 (3), 10.015 (2), 7.201 (2)	10.183 (1), 10.183 (1), 10.796 (1)
β (°)	90.00	90.00	95.28 (2)	90.00
V (Å^3)	1278.4 (4)	1266.3 (3)	1315.7 (5)	969.49 (16)
Z	8	8	8	6
D_x (Mg m^{-3})	1.207	1.219	1.173	1.194
Radiation type	Mo $K\alpha$	Mo $K\alpha$	Mo $K\alpha$	Mo $K\alpha$
μ (mm^{-1})	0.09	0.09	0.09	0.09
Crystal form, color	Plate (major faces are 001 and 110), colorless	Plate (largest face is 001), colorless	Lozenge (largest face is 100; others are 110 and 111), colorless	Block, colorless
Crystal size (mm)	0.32 × 0.25 × 0.06	0.30 × 0.25 × 0.08	0.50 × 0.33 × 0.17	0.20 × 0.20 × 0.20
Data collection				
Diffractometer	Nonius KappaCCD	Nonius KappaCCD	Nonius KappaCCD	Nonius KappaCCD
Data collection method	φ and ω scans with 1.0° steps	φ and ω scans with 2.0° steps	φ and ω scans with 1.0° steps	φ and ω scans with 2.0° steps
Absorption correction	Multi-scan (based on symmetry-related measurements)	Multi-scan (based on symmetry-related measurements)	Multi-scan (based on symmetry-related measurements)	Multi-scan (based on symmetry-related measurements)
T_{min}	0.98	0.97	0.97	0.98
T_{max}	0.99	0.99	0.99	0.98
No. of measured, independent and observed reflections	2046, 1124, 915	2001, 1099, 976	2102, 1159, 950	4834, 677, 620
Criterion for observed reflections	$I > 2\sigma(I)$	$I > 2\sigma(I)$	$I > 2\sigma(I)$	$I > 2\sigma(I)$
R_{int}	0.027	0.014	0.013	0.034
θ_{max} (°)	25.0	24.9	25.0	25.0
Refinement				
Refinement on	F^2	F^2	F^2	F^2
$R[F^2 > 2\sigma(F^2)]$, $wR(F^2)$, S	0.047, 0.101, 1.14	0.034, 0.086, 1.08	0.039, 0.102, 1.05	0.033, 0.076, 1.08
No. of reflections	1124	1099	1159	677
No. of parameters	75	75	90	76
H-atom treatment	Constrained to parent site	Constrained to parent site	Constrained to parent site	Constrained to parent site
Weighting scheme	$w = 1/[\sigma^2(F_o^2) + (0.037P)^2 + 0.24P]$, where $P = (F_o^2 + 2F_c^2)/3$	$w = 1/[\sigma^2(F_o^2) + (0.038P)^2 + 0.34P]$, where $P = (F_o^2 + 2F_c^2)/3$	$w = 1/[\sigma^2(F_o^2) + (0.042P)^2 + 0.4P]$, where $P = (F_o^2 + 2F_c^2)/3$	$w = 1/[\sigma^2(F_o^2) + (0.033P)^2 + 0.18P]$, where $P = (F_o^2 + 2F_c^2)/3$
$(\Delta/\sigma)_{max}$	< 0.0001	< 0.0001	< 0.0001	< 0.0001
$\Delta\rho_{max}$, $\Delta\rho_{min}$ (e Å^{-3})	0.17, −0.18	0.12, −0.20	0.12, −0.13	0.13, −0.11
Extinction method	None	None	None	*SHELXL*
Extinction coefficient	–	–	–	0.039 (6)

Computer programs used: *COLLECT* (Nonius, 1999), *SCALEPACK* (Otwinowski & Minor, 1997), *DENZO-SMN* (Otwinowski & Minor, 1997), *SHELXS*97 (Sheldrick, 1997*a*), *SHELXL*97 (Sheldrick, 1997*b*), *Mercury* (Macrae *et al.*, 2006) and local procedures.

source. Those data allowed determination of the absolute structure, which showed that the crystal we had used contained the *S*,*S* enantiomer (see below).

Most of the hydroxyl H atoms could be found in difference-Fourier maps. In the refinements the bond lengths (0.84 Å) and angles (109.5°) involving hydroxyl H atoms (unless not included; see below) were fixed, but the torsion angle around the adjacent C—O bond was allowed to vary [instruction AFIX 147 in *SHELXL*97 (Sheldrick, 1997*b*)]. All other H atoms were in calculated positions and allowed to ride on the attached C atom (AFIX 13, 23, or 43 as appropriate). Isotropic displacement parameters for all non-hydroxyl H atoms were 1.2 times larger than the U_{iso} of the attached C atom; the multiplicative factor for H atoms attached to O atoms was 1.5.

Displacement ellipsoids for the two structures of 2,3-TD at 90 K and the four structures of 1,2-CHD at 173 K are shown in Figs. 4 and 5. Displacement ellipsoids for the other six structures are available in the supplementary material.

3.1. 1:1 Compound of *cis*- and *rac*-2,3-tetralindiol

Numerous attempts were made over many years to grow crystals (from toluene, methanol, ethanol, 2-propanol, acetone, methylethyl ketone and water) using a small sample of the compound provided by A. Collet and a larger sample synthesized by M. Stiles. Crystals were always very small and often grew as clusters of exceptionally thin blades.

Data were first collected in 1997 at 110 (2) K on a Nonius CAD4 diffractometer with Mo $K\alpha$ radiation from a crystal having the dimensions 0.8 × 0.06 × 0.02 mm. Only 259 of the 1250 unique reflections having $\theta \leq 22.5^\circ$ ($\sin\theta/\lambda \leq 0.538$ Å^{-1}) had $I > 2\sigma(I)$, but the structure could be solved, albeit with difficulty, using the program *PATSEE* (Egert & Sheldrick, 1985) and a 2,3-TD search fragment. A highly constrained refinement gave poor agreement factors, but the structure was so logical (see Fig. 6) that we knew it must be basically correct.

Data were collected again in 1999 at 110 (2) K on a Nonius KappaCCD diffractometer with Mo $K\alpha$ radiation from a crystal having the dimensions 0.30 × 0.022 × 0.005 mm. Of 1244 unique reflections having $\sin\theta/\lambda \leq 0.538$ Å^{-1} 1081 had $I > 2\sigma(I)$. Because the refinement was still very unsatisfactory ($R_1 > 0.15$), the data in the frames were transformed with the program *PRECESSION* (Nonius, 1999) to give undistorted views of slices $nk\ell$, $hn\ell$ and hkn, n = 0–3 of the reciprocal lattice. These slices revealed that the crystal was twinned so that one axis, the c^* axis, had two orientations. In addition, a difference-Fourier map revealed a disorder of *cis* and *trans* molecules. Re-integration of the frames followed by incorporation of a twin model and split-atom models for two of the four O atoms (see Fig. 4) improved the refinement, but the R factor never went below 0.11 and the displacement ellipsoids were quite eccentric.

In 2005 data were collected once again for a crystal of similar size (0.30 × 0.05 × 0.02 mm) at 90.0 (2) K to 0.594 Å^{-1} on a Bruker–Nonius X8 Proteum diffractometer that used Cu $K\alpha$ radiation and that was equipped with a CRYOCOOL-LN2 low-temperature system (CRYO Industries of America, Manchester, NH). The data were integrated using a stand-alone version of *SAINT-Plus* (Bruker–Nonius, 2004), which can accommodate up to four separate crystal domains. Data scaling, merging of equivalents and correction for anisotropic absorption were performed with the *TWINABS* program (Sheldrick, 1999), which is essentially a multi-component variant of *SADABS* (Sheldrick, 1996). The refined twin matrix that premultiplies h_1 (Miller indices for component 1) to give h_2 is (−1.145 −0.011 −1.002/0.000 1.000 −0.001/1.002 −0.001 0.003). This matrix corresponds to a pseudotwofold axis around c of component 1, but the twin matrix could have just as well been chosen to correspond to a pseudotwofold rotation around a^* or a pseudomirror plane perpendicular to c or a^*. The axes b and c of the two components are parallel, as are the axes a^* and c^*. The value 1.145 is equal to $c^*\cos\beta^*/a^*$; the other values that are neither 0 nor ±1 probably reflect experimental uncertainties.

Reciprocal-lattice slices were again reconstructed from the measured frames; these slices showed the twinning clearly. These slices also revealed weak, but obvious, diffuse scattering parallel to a^* and c^* that was visible because of the greater than 10^3-fold increase in recordable diffracted X-rays in going from a sealed-tube Mo $K\alpha$ source to a focused (graded multilayer optics) rotating-anode Cu $K\alpha$ source. This diffuse scattering is much more prominent when k is odd than when k is even. No structured diffuse scattering was observed in planes $hn\ell$, n = 0–3. These observations suggest planes of weak diffuse scattering perpendicular to b^* for k odd. It seems likely that the diffuse scattering is associated with the disorder of the O atoms.

The largest faces of the crystal were identified, using the video camera on the diffractometer, as {001}; the crystals are therefore thinnest along c^*. The crystals are longest along **b**,

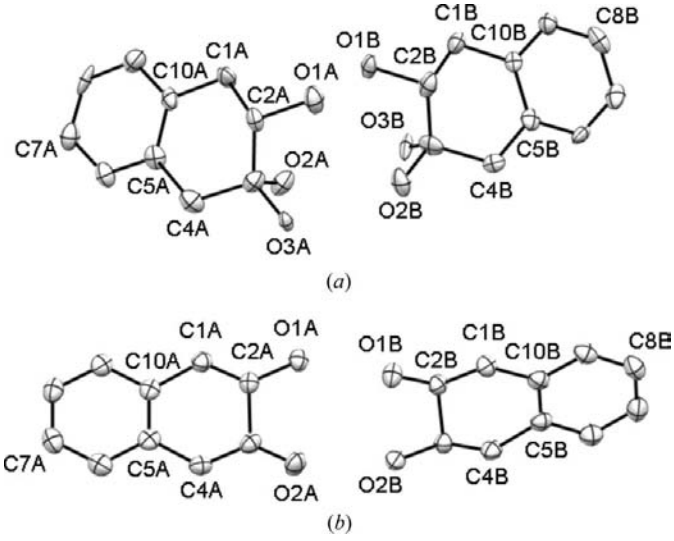

Figure 4
Perspective views of the asymmetric units of the 2,3-tetralindiol structures as determined at 90.0 (2) K. The displacement ellipsoids are drawn at the 70% level. H atoms have been omitted for the sake of clarity. Atoms are numbered in sequence around the rings; atom labels not shown can be worked out from those given. (*a*) The 1:1 compound of *cis*- and *trans*-2,3-tetralindiol (space group $C2$; $Z' = 2$). The disorder at the C3 atoms is shown. (*b*) *S*,*S*-2,3-Tetralindiol (space group $P2_1$, $Z' = 2$).

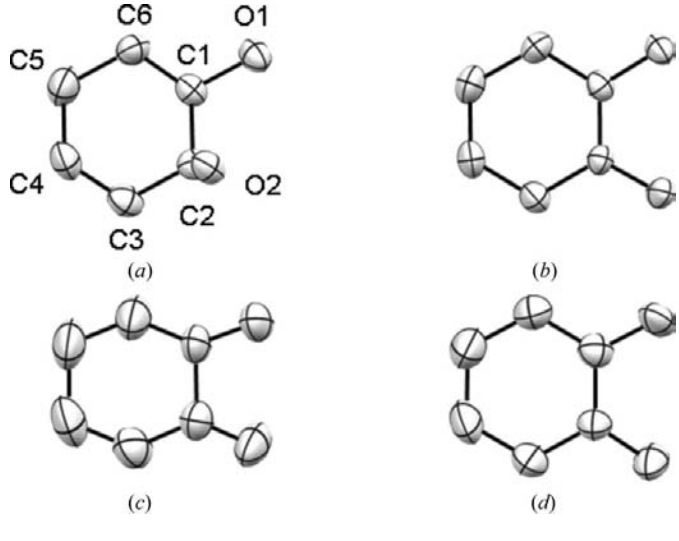

Figure 5
Perspective views of the asymmetric units of the 1,2-cyclohexanediol structures as determined at 173 (2) K. The displacement ellipsoids are drawn at the 70% level. H atoms have been omitted for the sake of clarity. The atom-numbering scheme is the same for all structures. (*a*) *cis*-1,2-Cyclohexanediol (*Pbca*); (*b*) *rac*-1,2-cyclohexanediol, *Pbca* polymorph; (*c*) *rac*-1,2-cyclohexanediol, $C2/c$ polymorph; (*d*) *R*,*R*-1,2-cyclohexanediol ($P3_221$).

which is the direction along which molecules are connected by hydrogen bonds.

Idealized views of the crystal structure as it would be if it contained only one *trans* enantiomer and were fully ordered are shown in Fig. 6. There are two crystallographically independent sites and in the crystals studied the *cis* and *trans* molecules are disordered at both of them. The *T*–*X* diagram (Lettré & Lerch, 1952; see Fig. 2) indicates that the overall composition is not necessarily exactly 1:1, so initially the occupancy factors for the two sites were refined independently. The two values obtained were so similar, however, that the two occupancy factors were made equal in the final least-squares cycles; the value at convergence was 0.609 (10). This result means that the crystal contained essentially equal numbers of *cis* and *trans* isomers, but that the ratio of the two *trans* enantiomers was about 3:2. The volume fraction of the larger twin component was determined to be 0.745 (2).

The H atoms attached to the ordered O atoms, which are located on the outer edges of the hydrogen-bonded stacks (see Fig. 6) could be located in a difference map. The H atoms attached to the disordered O atoms near the centers of the stacks were not included in the refinement because each would be disordered over at least four sites and no occupancy factor would be greater than 0.31. The twinning precluded averaging in C2 and meant that no absolute structure could be assigned.

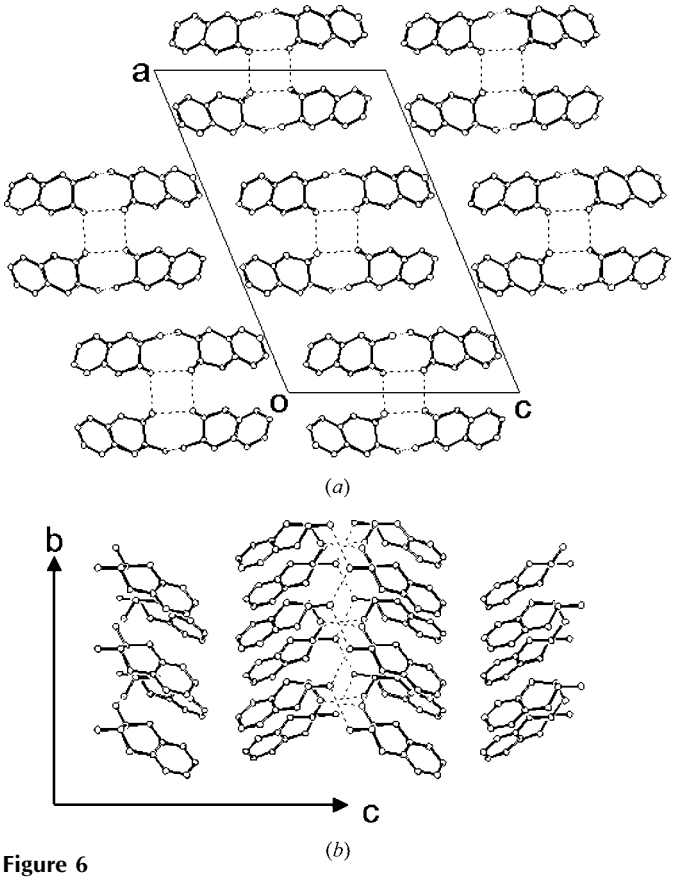

Figure 6
(*a*) Projection down the *b* axis of the idealized (*i.e.* fully ordered) structure of the 1:1 compound of *cis*- and one of the enantiomers of *trans*-2,3-tetralindiol. (*b*) Projection of part of a slice of the idealized structure. The slice is perpendicular to **a***.

The final structure is not entirely satisfactory by the standards used to assess typical non-disordered, non-twinned structures of small molecules. The average uncertainty for the bond lengths in the ordered parts of the molecules (0.008 Å) is relatively large and distances expected to be the same vary to a corresponding degree. Some of the displacement ellipsoids (see Fig. 4) are too small and some are too eccentric. There is no doubt, however, about the overall structure and the refinement problems are no surprise given the many crystallographic complications (very small crystal size, twinning, disorder and diffuse scattering). No restraints (other than that to fix the origin along **b**) were used.

3.2. *S,S*-2,3-Tetralindiol

This $P2_1$, $Z' = 2$ structure had been determined previously (Brianso, 1976; Lloyd *et al.*, 1998) but was redetermined at 90.0 (2) K [and earlier at 110 (2) K] so that the molecular volume *V*/*Z* could be better compared with that of the *cis*/*trans* compound. The structure was also determined at 173 (2) K for comparison with the 1,2-CHD structures. The positions of the hydroxyl H atoms at 90 K are much more reliable than those determined previously at room temperature.

Crystals in the form of thick tablets were grown without difficulty from toluene using resolved material provided by A. Collet and labeled '(+)'. Data were collected at 90.0 (2) K with a Bruker–Nonius X8 Proteum diffractometer using focused (graded multi-layer optics) Cu $K\alpha$ radiation from a rotating-anode source for a crystal 0.12 × 0.10 × 0.08 mm in size that had been cut from a larger crystal. The absolute structure was determined initially by refinement of the Flack parameter (see Table 3) with unmerged data. The resulting *S*,*S* configuration is the same as that already in the CSD. Later the configuration was checked by the Parsons/Flack quotient method (Parsons & Flack, 2004) using a special version of Sheldrick's *XPREP* program (Bruker AXS, 2006). The value of $x(u)$ was −0.03 (5).

3.3. *rac*-2,3-Tetralindiol?

A small sample of racemic material was provided by A. Collet. Numerous recrystallization attempts (from toluene, methanol, ethanol, 2-propanol, acetone, methylethyl ketone and water) failed to produce a single crystal that gave more than a few diffraction peaks that could be measured at 173 (2) K with a Nonius KappaCCD diffractometer and Mo $K\alpha$ radiation.

Most crystals grown were very thin, squarish plates that sometimes appeared twinned when viewed under a polarizing microscope. We were never able to measure a diffraction pattern that could be reliably indexed for crystals of this type.

A few block-like crystals gave good, but sparse, diffraction patterns with an apparent *C*-centered orthorhombic cell of dimensions 7.438 (1), 47.520 (5) and 28.086 (3) Å at 173 (2) K. If examined closely most of these crystals showed re-entrant angles. Transformation of this centered orthorhombic cell by (−7/12 −1/12 0/0 0 1/−5/12 1/12 0) gives dimensions *a*, *b*, *c* of 5.874, 28.086, 5.029 Å and angle β of 94.34°, which are essentially the same as those determined for the $P2_1$ structure

at 173 K (see Table 3). After this transformation only a very few reflections had both measurable intensity and non-integral indices; the diffraction pattern was therefore identified as arising from enantiomerically pure domains in two different orientations. The twin operation reverses the [101] direction of the $P2_1$ cell.

Two studies (Lettré & Lerch, 1952; Brianso, 1976) have indicated the existence of *rac*-2,3-TD with a melting point a few degrees higher than the eutectic temperature of *rac*-2,3-TD and *R*,*R*- (or *S*,*S*-) 2,3-TD. In an earlier paper (Lloyd *et al.*, 1998) we reported dimensions for a possible triclinic cell having a volume consistent with the presence of four *rac*-2,3-TD molecules, but we were neither able to solve the structure from that very limited data nor to find another crystal of the same type that gave a diffraction pattern that could be indexed.

3.4. *C*2/*c* polymorph of *rac*-1,2-cyclohexanediol

Crystals were grown by evaporation from acetone over a period of 2 d as tablets with pointed ends. Bounding planes appear to be {100}, {110} and {11$\bar{1}$ }. The crystals sublime; data collected at 299 (2) K over a period of 5 h showed a linear decrease in frame scale factor with time of 25%. Change in frame scale factor with time for data collected at 173 (2) K over a period of 2 h was, however, minimal.

Refinement of an ordered model for the data collected at 173 (2) K converged with agreement factors R_1 and wR_2 of 0.075 and 0.209; a difference-Fourier map showed three peaks of heights > 0.40 e Å^{-3} as well as a number of smaller peaks. The peaks appeared to define a second, enantiomeric molecule for which the O atoms were nearly coincident with those of the first. Refinement of a model including a rigid group for the minor component lowered R_1 and wR_2 to 0.039 and 0.102. The occupancy factor for the minor component is the same at the two temperatures [0.062 (2) and 0.068 (3) at 173 and 299 K] as is expected since the same crystal was used.

3.5. Enantiomerically pure and racemic (*Pbca* polymorph) *trans*-1,2-cyclohexanediol; *cis*-1,2-cyclohexanediol

Coordinates at 215 K for the structure of the resolved *trans* isomer of 1,2-CHD, which was incidental to a study of alcohol-amine complex formation, had been deposited (PIWXIK; Hanessian *et al.*, 1994), but the structure was not discussed. The structures at room temperature of *rac*-1,2-CHD (ZZZKPE01; Sillanpää *et al.*, 1984; ZZZKPE02; Jones *et al.*, 1989) and *cis*-1,2-CHD (ZZZPSA; Sillanpää *et al.*, 1984) had also been published. We redetermined all these structures at room temperature and at 173 K so that all the 1,2-CHD phases could be compared at similar temperatures. Sublimation during room-temperature data collection was substantial (18% for the enantiomerically pure crystal, 12% for the racemic crystal and 28% for the *cis* crystal), but was linear and so was corrected satisfactorily by the frame-to-frame scaling procedure. No sublimaton was observed during data collection at 173 K.

4. Analyses of 1,2-cyclohexanediol phases by powder diffraction

Samples (approximately 1 g) of 1,2-CHD crystals were grown at room temperature by evaporation of solutions of the pure *cis* (Pfaltz & Bauer), pure *rac* (Aldrich) and 1:1 stoichiometric mixtures of *cis* and *rac*-1,2-cyclohexanediol. Each sample was ground until it passed a 200 mesh sieve. Powder samples were poured into a 18 × 20 × 1.6 mm glass-backed aluminum sample well and leveled with a razor blade.

Data were collected digitally at room temperature on a Rigaku Geigerflex D/max vertical goniometer diffractometer with horizontal symmetrical reflection geometry and the Bragg–Brentano focusing condition. The X-ray source was a fixed-anode Cu $K\alpha$ tube, operating at 35 kV and 20 mA, with a graphite monochromator. The instrument was configured with 0.5° divergence and scatter slits and a 0.3 mm receiving slit. Two initial 30 min low-angle data collections, with the sample repacked between them, were compared to verify that sample graininess and differences in preferred orientation caused by loose packing did not substantially alter the observed pattern. Grinding and repacking was repeated until satisfactory agreement between the two test patterns was achieved. Data were collected over the range 10–80° 2θ in 0.05° θ steps, with a counting time of 3 s per step (*ca* 75 min total).

Intensities were corrected for absorption (Klug & Alexander, 1974) and fit using the DBWS-9006PC Rietveld refinement program (Sakthivel & Young, 1993) to the known phases (*i.e.* the cell dimensions, atomic coordinates and U_{iso} values) of *cis*-1,2-CHD (Sillanpää *et al.*, 1984) and *rac*-1,2-CHD (Sillanpää *et al.*, 1984; this work). Variables included a sample-height parameter and four background parameters for the sample as a whole; for each phase present a scale factor, overall Debye–Waller parameter and three peak-profile parameters were also varied. Preferred-orientation parameters were varied in initial cycles but did not improve the fit significantly; the final cycles included no correction for preferred orientation. Atoms refined anisotropically in the original structure determinations were assigned averaged isotropic displacement parameters. The overall Debye–Waller parameters accounted for the widening of atomic distributions caused by the grinding of these soft materials.

The weight fractions W for the phases were determined from the Rietveld scale factors S, the numbers Z and weights W of the formula units per unit cell and volumes V for each phase according to the formula (Young, 1993)

$$W_P = \frac{S_p(ZMV)_p}{\sum_i S_i(ZMV)_i}.$$

The average estimated standard uncertainty for a weight fraction (W) was approximately 3%.

Typical examples of observed, calculated and difference patterns of *cis*, *rac* and 1:1 *cis*:*rac*-*trans*-1,2-CHD are shown in Fig. 7. A table giving details of the refinements has been deposited.

5. Results

5.1. Disorder and hydrogen bonding in the *cis*/*trans* compound

The 1:1 *cis*/*trans* compound of 2,3-tetralindiol (see Fig. 6) consists of hydrogen-bonded stacks of molecules located on sites of symmetry 2, with each full stack being composed of four substacks in which molecules are related by translation along **b**. On the two longer sides of each stack, *i.e.* in planes parallel to {100}, the hydroxyl groups on the outside (O atoms O1*A* and O1*B* that are attached to C1*A* and C1*B*) form zigzag chains of hydrogen bonds. In the center of the stack, around the twofold axis parallel to **b**, the disordered hydroxyl groups (O atoms O2*A*, O3*A*, O2*B* and O3*B* that are attached to atoms C2*A* and C2*B*) can form hydrogen bonds in a number of ways [see part (*a*) of Fig. 8 and Table 5], although the number of hydrogen-bonding possibilities is much smaller than it first appears because half the O-atom sites must be empty. Each O-atom site is approximately equidistant from three other O-atom sites (O···O range 2.70–2.76 Å; see Table 5); all O···O···O angles are *ca* 90° (range 83–92°) and are staggered with respect to the bonds around C3*A* or C3*B*.

If only one enantiomer of the *trans* isomer were present then the hydrogen bonding in the center of the stack would be as shown in part (*b*) of Fig. 8. If only one *trans* enantiomer is present two of the four substacks are composed of *cis* isomers only and the other two substacks are composed of *trans* isomers only. Manipulations using the overlay feature available in *Mercury* (Macrae *et al.*, 2006) show that if there is only one *trans* enantiomer present then it cannot fit into the *cis* substack and there can be no disorder of the hydroxyl O

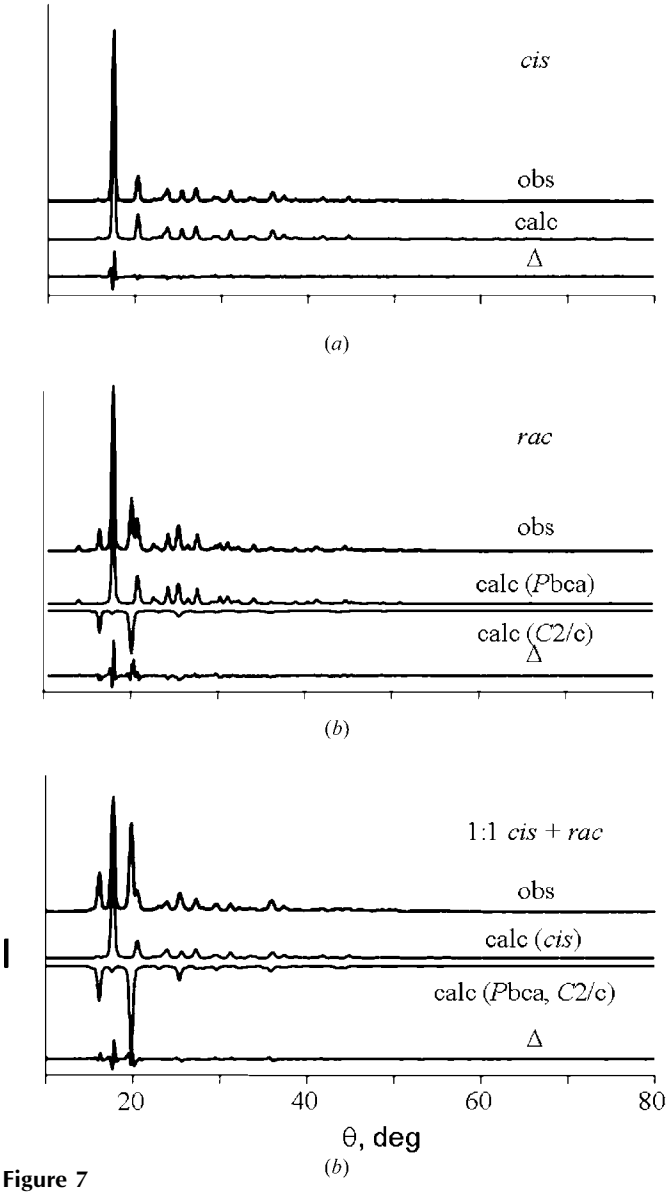

Figure 7
Observed and calculated powder patterns for recrystallized samples of 1,2-CHD. (*a*) The observed pattern of the *cis* isomer as fit by the one known phase (space group *Pbca*). (*b*) The observed pattern of the compound of the *R*,*R* and *S*,*S* enantiomers as fit by a combination of its two known racemic polymorphs. The peaks for the *C*2/*c* polymorph have been inverted to facilitate comparisons. (*c*) The observed pattern for samples recrystallized from a solution equimolar in the *cis* and *rac* isomers as fit by the three phases shown in parts (*a*) and (*b*) of the figure. The peaks for the *rac* polymorphs have been inverted to facilitate comparisons. We find no evidence for the presence of a significant amount of any other phase.

Table 5
Hydrogen-bond parameters (Å and °) as determined for the 2,3-tetralindiol structures at 90 K and the 1,2-cyclohexanediol structures at 173 K.

Atoms	O—H	H···O	O···O	O—H···O
2,3-Tetralindiols				
cis/*trans* compound (*C*2)				
In chain O1*B*···O1*A*	0.84	1.93	2.762 (7)	174
O1*A*···O1*B*	0.84	1.96	2.788 (7)	168
In $R_4^4(8)$ ring			2.723 (14)	
within dimer O3*A*···O3*B*				
O2*A*···O2*B*			2.760 (9)	
between dimers O3*B*···O3*A*			2.716 (14)	
O2*A*···O2*B*			2.747 (10)	
between rings O2*B*···O3*B*			2.708 (14)	
O2*A*···O3*A*			2.696 (14)	
S,*S* ($P2_1$)				
Within dimer O2*A*···O2*B*	0.84	2.03	2.855 (2)	166
in chain O1*B*···O1*A*	0.84	2.03	2.865 (2)	171
between dimers O2*B*···O1*A*	0.84	1.97	2.798 (2)	166
in chain O1*A*···O1*B*	0.84	1.96	2.799 (2)	174
C9*A*—H9*A*···O2*A*	0.95	2.45	3.384 (2)	168
1,2-Cyclohexanediols				
rac (*Pbca*)				
within dimer O1···O2	0.84	1.90	2.717 (1)	163
between dimers O2···O1	0.84	1.92	2.756 (1)	177
rac (*C*2/*c*)†				
within dimer O2···O1	0.84	1.91	2.727 (2)	164
between dimers O1···O2	0.84	1.86	2.693 (2)	171
R,*R* ($P3_22_12$)				
within dimer O2···O1	0.84	1.97	2.787 (2)	166
between dimers O1···O2	0.84	1.91	2.741 (2)	169
cis (*Pbca*)				
within dimer O2···O1	0.84	2.00	2.758 (1)	150
between dimers O1···O2	0.84	1.91	2.745 (1)	171

† Values given for major component only.

atoms. The hydrogen-bonded stack as viewed along **b** would then be described as

$$\begin{matrix} cis & R,R \\ R,R & cis \end{matrix} \quad \text{or as} \quad \begin{matrix} S,S & cis \\ cis & S,S \end{matrix}$$

The 'wrong' *trans* enantiomer can, however, fit into a *cis* substack, in which case the 'other' O site is occupied. Incorporation of the 'wrong' enantiomer in a *cis* substack changes the position of the hydroxyl group that is attached to atom C2 (close to the center of the hydrogen-bonded stack) and leads to disorder.

Inclusion of the wrong enantiomer in a *cis* substack results in the breaking of more hydrogen bonds than are formed. The hydrogen-bond pattern is disrupted least if the *cis* isomers are added at the same time to the *trans* substack so that the original pattern is restored except for a change of enantiomer. An example of how this might happen is shown in part (*c*) of Fig. 8.

The presence of both enantiomers within a single stack is not, however, necessary to explain the observed disorder. Since the overall profile of the stack is changed very little by the change from

$$\begin{matrix} cis & R,R \\ R,R & cis \end{matrix} \quad \text{to} \quad \begin{matrix} S,S & cis \\ cis & S,S \end{matrix}$$

there is no reason that two adjacent stacks should have the same composition.

The reconstructed reciprocal lattice slices show that the structure is also macroscopically twinned. Either the a^* axis is reversed and the b^* axis is unaffected or the a^* axis is unaffected and the b^* axis is reversed; in either case the axis c^* has two orientations. In direct space the b and c axes for the two domains are parallel, but the a axis has two orientations. The twinning could result from a twofold rotation around, or a mirror perpendicular to, c or a^*. A mirror plane seems more likely since it would preserve the herringbone arrangment shown in part (*b*) of Fig. 6. An overlay of two mirror-related hydrogen-bonded stacks shows that they are essentially identical except for a *ca* 6° rotation around **b**. The transformation (2 0 1/0 1 0/0 0 1) gives a new pseudo-orthombic cell with dimensions 42.98, 4.98, 15.48 Å and 90, 93.09, 90°. This angle β is quite far from 90°, but the failure of the crystals to grow well (except along **b**) suggests a significant misalignment.

It therefore seems likely that crystals grown from solutions or a melt equimolar in the *cis* isomer and one of the *trans* enantiomers would be both ordered and single. The twinning is probably a consequence of the presence of the second *trans* enantiomer.

5.2. Comparisons of the 2,3-tetralindiol structures

The structures of the *cis*/*trans* compound and of *S*,*S*- (and *R*,*R*-) 2,3-TD are surprisingly similar. Both are built from stacks of molecules that are related by translation (4.98 and 5.01 Å at 90 K), the important difference is the way these stacks are linked by hydrogen bonds (see Fig. 9). In both structures pairs of stacks are linked by a zigzag chain (atoms O1*A* and O1*B*); with the O···O distances (see Table 5) *ca* 0.05 Å shorter in the *cis*/*trans* compound. Furthermore, the projections of the stacks down the stacking axis are very similar [see part (*a*) of Fig. 9] and the stack of the *B* molecule

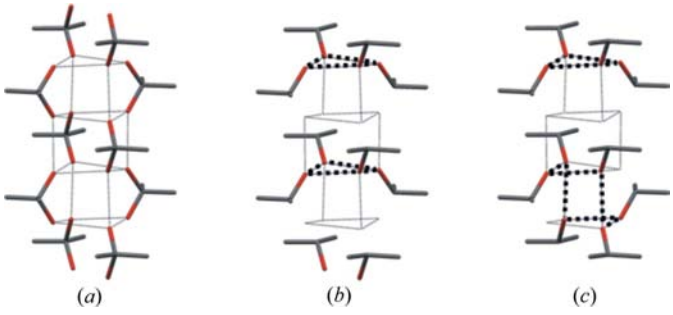

Figure 8
Possible hydrogen-bonding arrangements in the center of a molecular stack in the 1:1 compound of *cis* and *trans* 2,3-tetralindiol when both enantiomers of the latter can be present. Atoms C2, C3 and C4 are shown, as is one or both of the O atoms attached to C3. Gray lines indicated possible hydrogen bonds as identified in the fully disordered structure. (*a*) All possible positions of the hydroxyl O atoms attached to C3 are shown. (*b*) Hydrogen-bonding arrangement that would occur in the fully ordered compound between *cis*-2,3-tetralindiol and one of the pure enatiomers of *trans*-2,3-tetralindiol. (*c*) Hydrogen-bonding arrangement that could occur in a region in which *R*,*R*-2,3-tetralindiol molecules are replaced by the *cis* isomer, and the *cis* isomer is replaced by the *S*,*S* enantiomer.

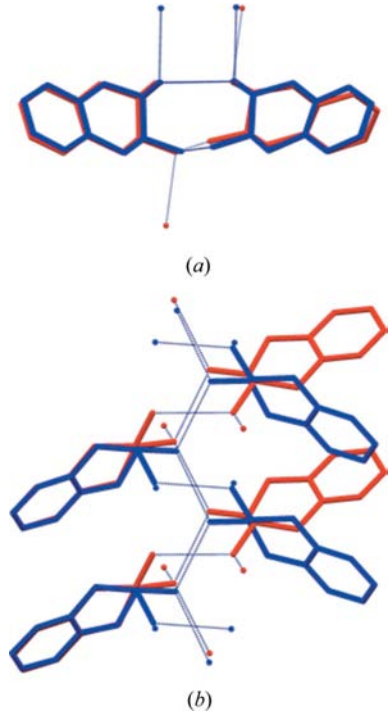

Figure 9
Projections of the stacks of 2,3-tetralindiol molecules in (blue) the fully ordered compound of *cis* and *R*,*R* molecules, and (red) the enantiomerically pure *trans* compound (*S*,*S* enantiomers). The molecules on the left are molecule *B* (*cis* isomer) of the compound and molecule *B* of the pure *S*,*S* enantiomer. (*a*) Projection down the stack. The view direction is **b** for the compound and **c** for the pure enantiomer. (*b*) Projections related to those in part (*a*) by a 90° rotation around the horizontal. The choice of enantiomer has little effect on the drawings.

of the compound and the stack of the *A* molecule of the *S*,*S* structure are nearly superimposable [see left-hand side of part (*b*) Fig. 9].

In the structure of the enantiomerically pure material, molecules in the two substacks are linked to form the dimer motif that is common in *vic*-diols (Brock, 2002). The pairs of substacks then form hydrogen bonds to two adjacent substacks to give layers in a way that is unremarkable except that the O1*A* atom is involved in three O—H···O bonds and the O2*A* atom is involved in only one. Interactions C9*A*—H9*A*···O2*A* (see Table 5) are probably also important.

In the structure of the 1:1 compound between *cis*-2,3-TD and a single 2,3-TD enantiomer it is almost certain (see above) that a dimer is also formed that is linked to another dimer by a $R_4^4(8)$ motif (notation of Bernstein *et al.*, 1995) centered on the twofold axis.

The packing in the *cis*-2,3-TD isomer (see Fig. 10) also has stacks composed of four substacks, but molecules adjacent in a substack are not in contact (spacing is 9.40 Å) and the hydrogen-bonding pattern is quite different.

In all three 2,3-TD structures there is at least one axial H atom from the saturated ring directed towards the center of the aromatic ring of an adjacent molecule.

5.3. 1,2-Cyclohexanediols

The *C*2/*c* modification of *rac*-1,2-CHD is closely related to the *Pbca* structures of both *rac*-1,2-CHD and *cis*-1,2-CHD. The topology of the hydrogen-bonding net (two-dimensional net of interlocking dimers; see Brock, 2002) is the same in the three structures (see Fig. 11); the structures differ in the orientation of the cyclohexyl rings relative to the hydrogen-bonded sheet and in the stacking of the sheets. The molecular volume of the *trans* isomer in the *C*2/*c* polymorph is 3.9% larger than in the *Pbca* polymorph at 173 K (3.7% at 299 K). The ratio of the average isotropic displacement parameter for the C atoms in *C*2/*c* and *Pbca* polymorphs is 1.71 at 173 K (1.49 at 299 K). The looser packing in the *C*2/*c* polymorph allows for a small amount (*ca* 6% for crystals grown at room temperature) of enantiomeric disorder. For *rac*-1,2-CHD precipitated from acetone at 295 (3) K (samples from four precipitations) the ratio of the *Pbca* and *C*2/*c* polymorphs was approximately 7:3.[4] A plausible explanation is that the *C*2/*c* polymorph is metastable relative to the *Pbca* polymorph at room temperature but is more easily nucleated.

The ratio of the molecular volumes in the *cis* and *trans Pbca* structures is 1.010 at 173 K and 1.008 at 299 K, with the *cis* molecule taking up slightly more space.

Crystals of enantiomerically pure 1,2-CHD are also built of dimers, but the two molecules in the dimer are related by a twofold rotation axis rather than an inversion center. Each dimer participates in hydrogen-bonded chains around two different threefold screw axes (space group $P3_221$ for the *R*,*R* enantiomer) so that the full hydrogen-bonding pattern is three-dimensional. At both 173 K and room temperature the molecular volume in this trigonal structure is 3 Å^3 larger than in the *Pbca* structure and 3 Å^3 smaller than in the *C*2/*c* structure. Since there is no sign of the $P3_121/P3_221$ structure in the powder patterns measured for *rac*-1,2-CHD, we conclude that this structure has a higher energy, perhaps because of its less favorable hydrogen bonding (see Table 5), than both the *Pbca* and *C*2/*c* structures.

The compound *S*,*S*-1,2-CHD is isostructural with (4*R*,5*R*)-1,2-dithiane-4,5-diol (Capasso & Zagari, 1981; refcode DTHDOM), in which C4, C5 and the attached H atoms of *S*,*S*-1,2-CHD are replaced by S atoms.[5] The survival of the packing arrangement and space group in the face of a rather large change to the molecular structure suggests that the hydrogen-bonding arrangement is structure determining.

We found no sign that any *cis–trans* solid-state compound of the 1,2-CHD molecules had formed. The powder-diffraction pattern of a sample precipitated at 295 (3) K from an ethanol solution equimolar in *cis*-1,2-CHD and *rac*-1,2-CHD was fit well by the known phases of the pure materials *cis*-1,2-CHD (*Pbca*), *rac*-1,2-CHD (*Pbca* and *C*2/*c*) in the ratios 0.56 (2):0.04 (2):0.40 (2). (The deviation from 0.50 of the *cis* fraction is an indication of the accuracy of the method.) We were somewhat surprised, however, to find that most of the *trans*-1,2-CHD had crystallized in the *C*2/*c*, rather than in the *Pbca*, structure. A second precipitation experiment gave similar results.

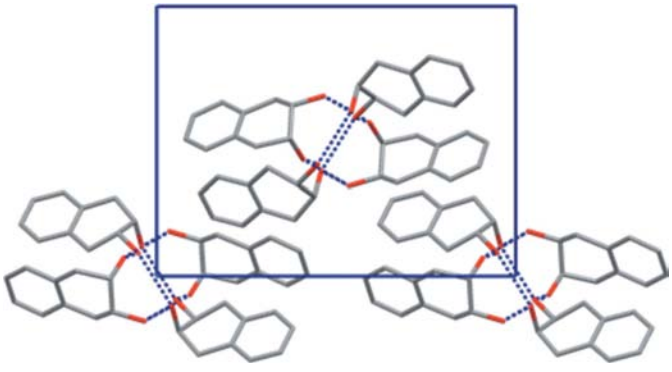

Figure 10
Packing in the structure of *cis*-2,3-tetralindiol (Klein *et al.*, 1983). The *b* axis is vertical and the *c* axis is horizontal.

6. Discussion

6.1. Compound or solid solution?

The experimental phase diagram determined by Lettré & Lerch (1952; see Figs. 1 and 2) shows a true 1:1 compound of *cis*-2,3-TD with one or the other of the *trans*-2,3-TD enantiomers, but a solid solution of the 1:1 *cis*/*R*,*R* and *cis*/*S*,*S* phases, which includes the 1:1 *cis*/*rac-trans* composition. The structure determination reported here is consistent with these

[4] These results essentially refute the rather unorthodox conclusion by Leitão *et al.* (2002) that the maximum in the *T–X* phase diagram of the enantiomers of *rac*-1,2-CHD corresponds to a solid solution.

[5] The change of S for CH_2 alters the numbering system of the ring and also alters the priority of the groups attached to the asymmetric centers; the *S*,*S*-cyclohexanediol therefore corresponds to the *R*,*R*-dithianediol

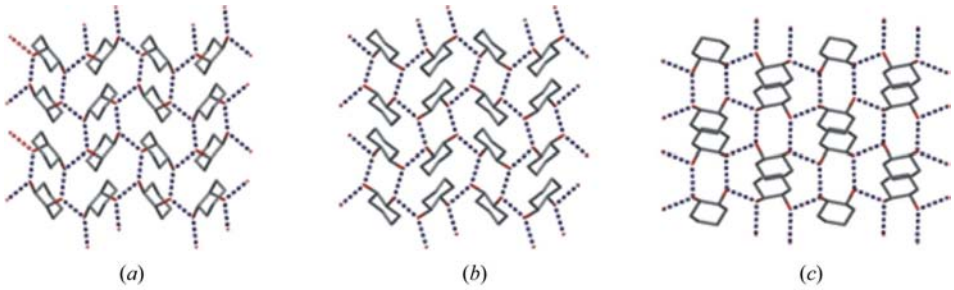

Figure 11
View of the hydrogen-bonded layers in the three structures of 1,2-cyclohexanediol: The topology of the hydrogen-bonded net is the same in all three: (*a*) the *cis* structure; (*b*) the *Pbca* polymorph of the *trans* isomer; (*c*) the *C*2/*c* polymorph of the *trans* isomer.

observations but provides somewhat different information about the disorder than does the thermodynamic study. The latter indicates that the volumes of ordered regions cannot be very large because existence of a solid solution implies that the disorder must be more like that of an uncountable number of small groups of molecules than like that of a small number of twin domains. The crystallographic work does not indicate the frequency of the enantiomer switches, but does show how they might happen.

6.2. Probability of compound formation

Crystals grown from multi-component solutions are expected to contain only one type of molecule (or cation/anion set) unless the two solutes are enantiomers or unless proton or electron transfer can occur between the two solutes. If compound formation in other situations were not rare then fractional crystallization would not be the method of choice for separations. Two factors are important in raising the probability of compound formation: compatibility of functional groups and the similarity of the other parts of the molecules.

Having two different molecules in the same crystal can be expected to lower packing efficiency. Consider the close packing of circles shown in part (*a*) of Fig. 12. If one of the circles is made smaller, as shown in part (*b*), then the spacing in the horizontal direction is appropriate for the larger circle but is too large for the smaller circle (*cf.* considerations of radius ratios in simple inorganic compounds). For the case of two molecules of somewhat different size this packing problem will be more difficult to draw and analyze, but will always be present. This packing problem also occurs if two crystallographically independent molecules of the same compound have quite different orientations.

This argument leads to the conclusion that larger asymmetric units are, on average, associated with lower packing efficiencies, and are therefore less probable. The argument echoes Pauling's (1929) 'Rule of Parsimony' for ionic crystals, which states that 'the number of essentially different kinds of constituents in a crystal tends to be small'.

Compound formation between isomers is therefore unexpected. The presence of both isomers in the asymmetric unit is unlikely to provide any special energy advantage, but is expected to lower the packing efficiency and thus raise the energy. If a compound does exist (such as that between *cis*- and *trans*-2,3-TD) then there is a good chance that there is some packing problem associated with the structure of one (or both) of the individual components that is solved in the compound.

6.3. Packing problem in 2,3-tetralindiol

The tetralindiol molecule is relatively small and rigid, and should form four O—H···O bonds. The small size means that the surface area is large relative to the molecular volume so that intermolecular contacts are relatively more important than in larger molecules. The rigidity means that there are few ways the molecule can adjust to improve those contacts. It is known that many *vic*-diols, $C_nH_m(OH)_2$, fail to form four O—H···O bonds because of competing packing requirements (Brock, 2002). In tetralindiol there is yet another problem, which is the small but significant thickness mismatch between the aromatic and aliphatic parts of the tetralin ring system. If the molecules are stacked so that tetralin fragments are related by translation, then the spacing appropriate for the aliphatic rings must be a little larger than is appropriate for the aromatic rings, which will be separated by small regions of empty space. Space-filling representations generated with the

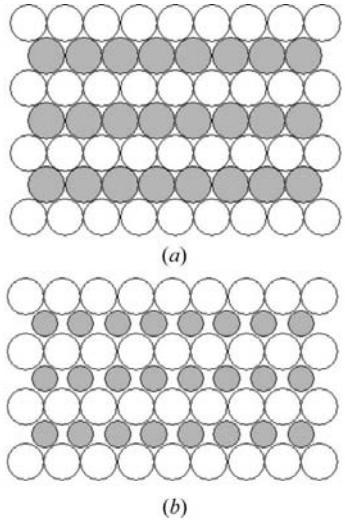

Figure 12
(*a*) A close-packed plane of circles, all of the same size. (*b*) A plane formed from circles having two different radii. The circles in the second plane fill space in some directions but not in others.

program *Mercury* (Macrae *et al.*, 2006) of the *S*,*S*-2,3-TD and *cis*/*trans* structures, both of which have such stacks, show this mismatch clearly.

The *cis*-TD structure avoids this mismatch problem to some extent by having pairs of molecules arranged head-to-tail, with the aromatic ring of one independent molecule over the aliphatic ring of the other. While this arrangement improves packing efficiency, it puts molecular regions that have quite different electronic properties in close proximity.

It is noteworthy that all three known TD structures have $Z' = 2$, but that all four CHD structures known have $Z' = 1$. We suspect, for reasons detailed above, that Z' values larger than 1 (or larger than $\frac{1}{2}$ in the case of centrosymmetric molecules; see Pidcock *et al.*, 2003) are indicative of packing problems.

6.4. Why no structure of *rac*-2,3-tetralindiol?

If the 2,3-TD system behaved as expected, a racemic compound of the enantiomers would be more stable than crystals of the *R*,*R* and *S*,*S* compounds. A key to understanding why the *cis*/*trans* compound dominates the phase diagram is understanding why the racemic compound fails to yield good crystals.

If crystals of the *rac*-2,3-TD structure exist, and there is reason to believe that they do (Lettré & Lerch, 1952), then we believe they grow as exceptionally thin flakes. That habit would be consistent with a structure that has a two-dimensional hydrogen-bonding pattern similar to that seen for the two polymorphs of *rac*-1,2-CHD, but in which interactions between the layers are so unfavorable that the crystals fail to grow well in the third dimension.

Why can't a good crystal of *rac*-2,3-TD be built from the hydrogen-bonding pattern seen for the two polymorphs of *rac*-*trans*-1,2-CHD? Examination of space-filling representations of the 1,2-CHD polymorphs shows that there are small regions of empty space between the cyclohexyl rings. The packing coefficients calculated by *PLATON* (Spek, 2003) for the 1,2-CHD structures are all low [0.668 and 0.647 for the *Pbca* and *C*2/*c* polymorphs, 0.657 for the *R*,*R* (or *S*,*S*) compound, and 0.663 for the *cis* compound, all at room temperature]. The small voids between the cyclohexyl rings exist because the hydrogen-bonding pattern favors molecular spacings that are larger than those that would lead to close packing of the cyclohexyl rings. Replacing the H atoms of C4 and C5 of the 1,2-CHD with a fused aromatic ring would magnify this packing problem because the appropriate spacing for the aromatic rings is even smaller than for the cyclohexyl rings. The difference in favorable spacings for the hydroxyl groups and aromatic rings is not large enough, however, to allow interpenetration of adjacent double layers. (Interpenetration of adjacent hydrogen-bonded ribbons is seen in the *cis*-2,3-TD structure). It can therefore be assumed that the packing coefficient for *rac*-2,3-TD would be even lower than for the *rac*-1,2-CHD polymorphs.

S,*S*- (and *R*,*R*-)-2,3-TD does have a two-dimensional hydrogen-bond arrangement and reasonably densely packed molecular double layers (packing coefficients 0.696 and 0.716 at room temperature and 90 K). That hydrogen-bond arrangement, however, is somewhat different than those seen in the 1,2-CHD polymorphs and is probably not optimal since the O1*A* atom is involved in three O—H···O bonds and the O2*A* atom is involved in only one. This variant pattern reduces the area per dimer in the hydrogen-bonded layer [from 32.8 and 36.1 Å^2 in the two CHD polymorphs to 29.6 Å^2 in *S*,*S*-2,3-TD, all at 173 K], but the aromatic rings in *S*,*S*-2,3-TD are still not in contact.

6.5. Advantages of the *cis*/*trans* 2,3-tetralindiol compound

The presence of two kinds of molecules in the *cis*/*trans* compound of 2,3-TD allows both a satisfactory hydrogen-bonding pattern and a satisfactory stacking arrangement of the aromatic and aliphatic rings. The two isomers are complementary. Each hydroxyl group can make two good O—H···O bonds and the molecules stack densely. Because both the isomers themselves and their orientations are so similar the spacing-mismatch problem associated with the presence of two different molecules is minimized.

The O···O distances (see Table 5) suggest that the O—H···O bonds in the *cis*/*trans* structure are better than in the *S*,*S* (or *R*,*R*) structure. The packing efficiency at 90 K in the compound (0.709) is also just a little smaller than for the *S*,*S* enantiomer (0.716). No direct comparison can be made between the structures of the 1:1 compound and of the *cis* isomer because it was not possible to do the structures at the same temperature, but the structure of the pure enantiomer is *ca* 1% denser at room temperature than that of the *cis* isomer, and is slightly denser than the compound at low temperatures. Comparisons of O···O distances suggests that the hydrogen bonding in the 1:1 compound is at least as good as in the *cis* isomer.

6.6. Closely related compounds

Efforts were made to find a *cis*/*trans* compound of 1,3-cyclohexanediol (Mueller, 1990), but none was discovered. There is, however, a 1:1 compound of *cis*- and *rac*-1,4-cyclohexanediol (Loehlin, 2006). A packing problem in the pure *rac* isomer of 1,4-CHD (refcodes POVSEY and POVSEY01; Steiner & Saenger, 1998, Chambers *et al.*, 2000) is obvious: the asymmetric unit has $Z' = 2$ and contains both the more favorable diequatorial and the less favorable diaxial conformer.

We know of two other compounds of *cis* and *trans* diol isomers. One contains the isomers of 1,6-cyclodecanediol (refcode VENZOD; Ermer *et al.*, 1989). The structures of the pure *cis* (refocde VENZIX; Ermer *et al.*, 1989) and *rac* (CDECOL11; Ermer *et al.*, 1973) isomers both have two molecules in the asymmetric unit, and one of the two molecules in the *cis* structure, which is isostructural with that of the *cis*/*trans* compound, is completely disordered. The second diol compound we know of is formed from the *cis* and *trans* isomers of 2,5-dimethyl-3-hexene-2,5-diol (refcode CTHXDL; Ruysink & Vos, 1974).

A number of compounds between 1,2-CHD and 1,2-diaminocyclohexane have been made (Hanessian *et al.*, 1994, 1995, 1999), several of which (refcodes PIWXOI and PIWXUO) have hydrogen-bonding arrangements similar to that seen in the *cis*/*trans* compound reported here.

7. Summary and conclusions

Compounds of stereoisomers are rare because the specific advantages of having two different molecules present (*e.g.* for the formation of hydrogen bonds) rarely offset the disadvantage of having two molecules for which the appropriate spacings are incompatible in at least one direction. The 1:1 compound of *cis*- and *trans*-2,3-tetralindiol is exceptional, because the isomers allow a hydrogen-bonding pattern that is more favorable than in the individual components while also allowing close packing of the molecules. The presence of two different molecules generates no spacing mismatch in this 1:1 compound because the nearly identical hydrocarbon parts of the two molecules are in essentially the same environment.

We suspect that the likelihood of compound formation is raised when strong hydrogen-bonding groups are present. Many *vic* diols, for example, do not manage to form a full set of O—H···O bonds in their crystals (Brock, 2002) and so are good candidates for compound formation.

Even though the formation of solid-state compounds from stereoisomers may be unexpected, its frequency may still have been underestimated. Chemists seldom grow crystals from solutions equimolar in two different molecules unless they are enantiomers. Second, it is difficult to recognize that a compound has been formed unless its melting point on a *T*–*X* phase diagram lies above the melting point curve for the higher-melting component. If the melting point lies below that curve but above the eutectic temperature of $A + B$, then complete evaporation of a solution that is equimolar in *A* and *B* should contain a mixture of crystals of the higher-melting component and of the compound, as well as the very small crystals of the eutectic mixture of the compound and lower-melting component. The presence of the compound might easily be missed. We expect that Rietveld analyses of the type described above would reveal more solid-state compounds of isomers than are currently known.

We are very grateful to the late Professor André Collet (Lyon) for providing the samples of [+]-*trans*-TD and *rac*-2,3-TD with which we began this project, and to Professor Martin Stiles for later synthesizing more of the *cis*/*trans* 2,3-TD compound. It is a pleasure to acknowledge many conversations with Professor J. D. Dunitz, who first brought the 2,3-TD compound to our attention. We thank Professor R. A. Young for his help and encouragement with the powder work. We thank Anita Coetzee and Rob Hooft, then of Nonius (Delft), for re-integrating the frames measured in 1999 to separate the contributions of the two twin components. We are grateful to a referee for some helpful suggestions. We are grateful to the Kentucky EPSCoR program (NSF Grant EHR-91-08764) for financial support, to the National Science Foundation (MRI No. 0319176) for funds to purchase the Bruker–Nonius X8 Proteum diffractometer and to the International Centre for Diffraction Data for a scholarship to M. A. Lloyd.

References

Ali, M. E. & Owen, L. N. (1958). *J. Chem. Soc.* pp. 1066–1073.
Allen, F. H. (2002). *Acta Cryst.* B**58**, 380–388.
Bernstein, J., Davis, R. E., Shimoni, L. & Chang, N.-L. (1995). *Angew. Chem. Int. Ed. Engl.* **34**, 1555–1573.
Brianso, M.-C. (1976). *C. R. Seances Acad. Sci. Sr. C*, **283**, 457–460.
Brock, C. P. (2002). *Acta Cryst.* B**58**, 1025–1031.
Brock, C. P., Schweizer, W. B. & Dunitz, J. D. (1991). *J. Am. Chem. Soc.* **113**, 9811–9820.
Bruker AXS (2006). *XPREP*, Version 2006/1. Bruker AXS, Madison, Wisconsin, USA.
Bruker–Nonius (2004). *APEX*2. Bruker-Nonius AXS, Madison, Wisconsin, USA.
Capasso, S. & Zagari, A. (1981). *Acta Cryst.* B**37**, 1437–1439.
Chambers, R. D., Diter, P., Dunn, S. N., Farren, C., Sandford, G., Batsanov, A. S. & Howard, J. A. K. (2000). *J. Chem. Soc. Perkin Trans. 1*, pp. 1639–1649.
Egert, E. & Sheldrick, G. M. (1985). *Acta Cryst.* A**41**, 262–268.
Ermer, O., Dunitz, J. D. & Bernal, I. (1973). *Acta Cryst.* B**29**, 2278–2285.
Ermer, O., Vincent, B. R. & Dunitz, J. D. (1989). *Isr. J. Chem.* **29**, 137–142.
Etter, M. C. (1990). *Acc. Chem. Res.* **23**, 120–126.
Etter, M. C. (1991). *J. Phys. Chem.* **95**, 4601–4618.
Flack, H. D. (1983). *Acta Cryst.* A**39**, 876–881.
Groth, P. (1910). *Chemische Kristallographie. Dritter Teil: Aliphatische und Hydroaromatische Kohlenstoffverbindungen*, Vol. 3. Leipzig: Engelmann.
Hanessian, S., Gomtsyan, A., Simard, M. & Roelens, S. (1994). *J. Am. Chem. Soc.* **116**, 4495–4496.
Hanessian, S., Saladino, R., Margarita, R. & Simard, M. (1999). *Chem. Eur. J.* **5**, 2169–2183.
Hanessian, S., Simard, M. & Roelens, S. (1995). *J. Am. Chem. Soc.* **117**, 7630–7645.
Herbstein, F. H. (1971). *Perspectives in Structural Chemistry*, edited by J. D. Dunitz & J. A. Ibers, Vol. IV, pp. 166–395. New York: John Wiley and Sons.
Herbstein, F. H. (2005). *Crystalline Molecular Complexes and Compounds*, 1st ed. Oxford University Press.
Jacques, J., Collet, A. & Wilen, S. H. (1981). *Enantiomers, Racemates and Resolutions*. New York: John Wiley & Sons.
Jones, P. G., Edwards, M. R. & Kirby, A. J. (1989). *Acta Cryst.* C**45**, 244–246.
Klein, C. L., Majeste, R. J., Tsang, W.-S., Griffin, G. W. & Stevens, E. D. (1983). *Acta Cryst.* C**39**, 1405–1407.
Klug, H. P. & Alexander, L. E. (1974). *X-ray Diffraction Procedures for Polycrystalline and Amorphous Materials*, 2nd ed. New York: Wiley-Interscience.
Leitão, M. L. P., Eusébio, M. E., Maria, T. M. R. & Redinha, J. S. (2002). *J. Chem. Thermodyn.* **34**, 557–568.
Leroux, H. (1909). *C. R.* **148**, 931–933 (Can: 3:11625).
Lettré, H. & Lerch, I. (1952). *Chem. Ber.* **85**, 394–397.
Lloyd, M. A., Patterson, G. E. & Brock, C. P. (1998). *Acta Cryst.* C**54**, 1486–1488.
Loehlin, J. H. (2006). Personal communication.
Macrae, C. F., Edgington, P. R., McCabe, P., Pidcock, E., Shields, G. P., Taylor, R., Towler, M. & van de Streek, J. (2006). *J. Appl. Cryst.* **39**, 453–457.
Mueller, B. (1990). Diplom Arbeit Thesis. Swiss Federal Institute of Technology.

Nonius (1999). *COLLECT*. Nonius BV, Delft, The Netherlands.
Otwinowski, Z. & Minor,W. (1997). *Methods Enzymol.* **276**, 307–326.
Parsons, S. & Flack, H. D. (2004). Abstracts of the European Crystallographic Meeting, Budapest.
Patrick, B. O. & Brock, C. P. (2006). *Acta Cryst.* B**62**, 488–497.
Pauling, L. (1929). *J. Am. Chem. Soc.* **51**, 1010–1026.
Pauling, L. & Delbrueck, M. (1940). *Science*, **92**, 77–79.
Pidcock, E., Motherwell, W. D. S. & Cole, J. (2003). *Acta Cryst.* B**59**, 634–640.
Ruysink, A. F. J. & Vos, A. (1974). *Acta Cryst.* **30**, 1997–2002.
Sakthivel, A. & Young, R. A. (1993). *User's Guide to Programs DBWS-9006 and DBWS-9006PC for Rietveld Analysis of X-ray and Neutron Powder Diffraction Patterns.* Georgia Institute of Technology, Atlanta, Georgia, USA.
Sheldrick, G. M. (1994). *SHELXTL PC.* Siemens Analytical Instruments, Inc., Madison, Wisconsin, USA.
Sheldrick, G. M. (1996). *SADABS.* University of Göttingen, Germany.
Sheldrick, G. M. (1997*a*). *SHELXS*97. University of Göttingen, Germany.
Sheldrick, G. M. (1997*b*). *SHELXL*97. University of Göttingen, Germany.
Sheldrick, G. M. (1999). *TWINABS.* University of Göttingen, Germany.
Sillanpää, R., Leskelä, M. & Hiltunen, L. (1984). *Acta Chem. Scand. Ser. B*, **38**, 249–254.
Spek, A. L. (2003). *J. Appl. Cryst.* **36**, 7–13.
Steiner, T. & Saenger, W. (1998). *J. Chem. Soc. Perkin Trans. 2*, pp. 371–378.
Verkade, P. E., Coops, J., Maan, C. J. & Verkade-Sandbergen, A. (1928). *Justus Liebigs Ann. Chem.* **467**, 217–239.
White, T. N. (1931). *Z. Kristallogr.* **80**, 5–17.
Young, R. A. (1993). *The Rietveld Method*, edited by R. A. Young. Oxford University Press.